



HAL
open science

The impact of fluid-dynamic stress in stirred tank bioreactors on the synthesis of cellulases by *Trichoderma reesei* at the intracellular and extracellular levels

Tamiris Roque, Jérôme Delettre, Nicolas Hardy, Alvin W Nienow, Frédéric Augier, Fadhel Ben Chaabane, Catherine Béal

► To cite this version:

Tamiris Roque, Jérôme Delettre, Nicolas Hardy, Alvin W Nienow, Frédéric Augier, et al.. The impact of fluid-dynamic stress in stirred tank bioreactors on the synthesis of cellulases by *Trichoderma reesei* at the intracellular and extracellular levels. *Chemical Engineering Science*, 2021, 232, pp.116353. 10.1016/j.ces.2020.116353 . hal-03137304v2

HAL Id: hal-03137304

<https://ifp.hal.science/hal-03137304v2>

Submitted on 13 Apr 2022

HAL is a multi-disciplinary open access archive for the deposit and dissemination of scientific research documents, whether they are published or not. The documents may come from teaching and research institutions in France or abroad, or from public or private research centers.

L'archive ouverte pluridisciplinaire **HAL**, est destinée au dépôt et à la diffusion de documents scientifiques de niveau recherche, publiés ou non, émanant des établissements d'enseignement et de recherche français ou étrangers, des laboratoires publics ou privés.

2

3 **The impact of fluid-dynamic stress in stirred tank bioreactors on the**
4 **synthesis of cellulases by *Trichoderma reesei* at the intracellular and**
5 **extracellular levels**

6

7 Tamiris Roque¹, Jérôme Delettre², Nicolas Hardy¹, Alvin W Nienow³, Frédéric Augier⁴, Fadhel
8 Ben Chaabane¹, Catherine Béal²

9

10 *1 IFP Energies Nouvelles, 1 et 4 avenue de Bois-Préau, 92852 Rueil-Malmaison, France;*

11 *2 AgroParisTech, UMR SayFood, 1 avenue Lucien Brétignières, 78850 Thiverval-Grignon, France;*

12 *3 School of Chemical Engineering, University of Birmingham, Edgbaston, Birmingham B15 2TT,*
13 *United Kingdom;*

14 *4 IFP Energies Nouvelles, Rond-Point de l'Echangeur de Solaize, BP3, 69360 Solaize, France*

15

16 **Corresponding author: frédéric.augier@ifpen.fr*

17

18 **Abstract**

19
20 Cellulases for bioethanol production are mainly made by fed-batch fermentation using a
21 filamentous fungus, *Trichoderma reesei*. Agitation at different scales impacts on
22 morphology, rheology and growth rate and can be correlated by $EDCF_{\epsilon_{max}}$. Typically,
23 $EDCF_{\epsilon_{max}}$ is much smaller at commercial scale and fungal size, viscosity and growth rate are
24 greater. Here, to increase understanding, continuous culture in 3 L bioreactors using two
25 $EDCF_{\epsilon_{max}}$ values were undertaken. The higher $EDCF_{\epsilon_{max}}$ decreased the cellulase production
26 (concentration, 21 %; specific production rate, 24 %; protein yield, 20 %) whilst proteomic
27 analysis showed, at an intracellular level, a decrease of cellulase and hemicellulase
28 synthesis. An increase of stress proteins also occurred, which may help cells to limit the
29 impact of fluid dynamic stress. Also, cellulase production during continuous culture at the
30 bench varied with $EDCF_{\epsilon_{max}}$ similarly to that between bench and commercial scale during
31 fed-batch culture.

32

33 **Key-words:** *Trichoderma reesei*; cellulases; fluid dynamic stress; scale-up/scale-down;
34 proteomic analysis.

35

36 **Highlights**

37

- 38 • Higher values of $EDCF_{\epsilon_{max}}$ reduce production of extracellular cellulases
- 39
- 40 • This reduction is linked to a lowering of intracellular synthesis of cellulases
- 41
- 42 • Higher fluid dynamic stress leads to the appearance of stress proteins
- 43
- 44 • Intracellular stress proteins induce moderate changes in q_p from large ones in $EDCF_{\epsilon_{max}}$
- 45

46 1. Introduction

47 Second-generation (2G) bioethanol from lignocellulosic materials is a good candidate
48 to replace conventional fuels. Indeed, 2G bioethanol allows a reduction of about 85% of
49 greenhouse gas emissions compared to fossil fuels (Morales et al., 2015). Also, 2G
50 bioethanol uses lignocellulosic waste from the agri-food and forestry and does not compete
51 with food. However, production costs remains high compared to ethanol from starch. This
52 increase is mainly due to the high price of cellulases, the enzymes which hydrolyze
53 lignocellulosic biomass into simple sugars. The 2G bioethanol price can be reduced if
54 cellulases production costs are lowered (Hardy et al., 2017). Economy of scale is a way of
55 doing so, requiring the use of bioreactors of several hundred cubic meters, a huge size
56 compared with that at which the process is developed. With increasing scale, the medium in
57 the bioreactor experiences increasing spatial heterogeneities (Amanullah et al., 2004; Lara
58 et al., 2006) and the fluid dynamic stresses change (Hardy et al., 2017); and it is important to
59 know what their impact will be.

60 Cellulolytic enzymes are mainly produced at industrial scale by the filamentous
61 fungus *Trichoderma reesei* because of its high cellulases secretion capacity (Ferreira et al.,
62 2014; Soni et al., 2018). As enzyme production is dissociated from growth, industrial
63 cultures are often carried out in two steps: a batch phase for growth of the fungus followed
64 by a fed-batch phase for the production of cellulases (Jourdier et al., 2013). During growth,
65 *T. reesei* can use different carbon sources, but glucose is the most common (Hardy, 2016).
66 As the *T. reesei* grows, it develops hyphae which form complex structures (Hardy et al.,
67 2017b). The complex morphology and high concentrations at the end of growth lead to a
68 high viscosity medium with shear thinning behaviour (Gabelle et al., 2012; Hardy et al.,
69 2015; Quintanilla et al., 2015).

70 The production phase starts when the growth stops by limiting the carbon source to
71 induce the production of cellulases (dos Santos Castro et al., 2014). In this phase, soluble
72 sugars such as sophorose, cellobiose and lactose are used to induce the secretion of
73 cellulases. In order to avoid further growth, an inductive substrate is fed continuously at an
74 optimal limiting rate (Jourdier et al., 2013; Hardy et al., 2017). As *T. reesei* is a strictly
75 aerobic microorganism, the dissolved oxygen concentration (dO_2) must be above the critical
76 value, 15 % dO_2 ($1.2 \text{ mg of } O_2 \cdot L^{-1}$) (Marten et al., 1996) for the strain RUT-C30. However, the
77 high viscosity at the end of the batch phase reduces mass transfer rates, and oxygen
78 transfer (Albaek et al., 2012; Gabelle et al., 2012). To ensure $dO_2 > 15 \% dO_2$ at this time, the
79 power input has to be increased (Gabelle et al., 2012), enhancing the fluid dynamic stress on
80 the mycelia.

81 There are many ways of characterizing fluid dynamic stress with changes in agitation
82 intensity and with scale (Amanullah et al., 2004). Until the 1990s, the two most common
83 were tip speed or specific power input, P/V ($W \cdot m^{-3}$). However, in 1996, it was shown with
84 the fungus, *P. chrysogenum*, that whilst tip speed increased with scale at constant specific
85 power, damage to the organism was reduced (Jüsten et al., 1996). However, a new function
86 which reduced with increasing scale, the energy dissipation/circulation function, *EDCF*, was
87 able to correlate fungal breakage and various growth parameters, better than P/V (Jüsten et
88 al., 1996). In essence, the *EDCF* concept is that fungus break to an equilibrium size
89 dependent on the maximum specific energy dissipation rate, ϵ_{max} ($W \cdot m^{-3}$) in a region close
90 to the impeller and the frequency with which the organism passes through that region, $1/t_c$
91 (s) where the circulation time, $t_c = V/(Fl \cdot N \cdot D^3)$. Here, V (m^3) is the volume of broth in
92 the bioreactor, N ($rev \cdot s^{-1}$) the agitator speed, D (m) its diameter and Fl (dimensionless), its
93 flow number. Because the circulation time increases with increasing scale even at constant

94 P/V , $EDCF$ generally decreases with scale, sometimes markedly. There are a number of
95 ways of assessing ε_{max} and a recently developed definition by Grenville et al. (2017) is
96 $\varepsilon_{max} = 1.04 \cdot x \cdot \rho \cdot Po^{\frac{3}{4}} \cdot N^3 \cdot D^2$. Here, x is the ratio of impeller diameter to trailing vortex
97 diameter, a dimensionless characteristic of the impeller being used, as is Po , the power
98 number; and ρ ($\text{kg}\cdot\text{m}^{-3}$) is the density of the broth. In 2017, we used this definition of
99 ε_{max} to develop (Hardy et al., 2017) an improved $EDCF$ function, $EDCF_{\varepsilon_{max}}$. We then used
100 $EDCF_{\varepsilon_{max}}$ to correlate the impact of the fluid dynamic stress associated with a variety of
101 impellers on various process parameters during the initial batch growth phase of *T. reesei*
102 fermentations at the bench scale and also with a multiple impeller combination at the
103 industrial scale.

104 Other filamentous organisms to which the $EDCF$ has been applied are *T. harzianum* (Rocha-
105 Valadez et al., 2007), *A. oryzae* (Amanullah et al., 2002) and *P. ostreatus* (Fernández-
106 Alejandro et al., 2016), where it was related to the transition of the organism from clumps
107 to pellets. With *T. reesei* (Hardy et al., 2017), higher values of $EDCF_{\varepsilon_{max}}$ reduced the mycelial
108 size and specific growth rate (by up to 20 %) at the bench scale whilst at the commercial
109 scale, as explained above, though the tip speed increased, $EDCF_{\varepsilon_{max}}$ decreased leading to
110 larger mycelia, higher viscosity and higher growth rates. However, as the bench runs were
111 limited to the growth phase, cellulases were not produced; so the impact of fluid dynamic
112 stresses on their production could not be investigated.

113 Previous work on the proteome of *T. reesei* has been studied in order to better
114 identify the enzymes involved in lignocellulosic biomass degradation and the protein
115 secretion profile under different environmental conditions (Herpoël-Gimbert et al., 2008).
116 Apart from the common proteins involved in general metabolism, it mostly consists of two
117 cellobiohydrolases (CBHI and CBH2), five endoglucanases (EGI, EGII, EGIII, EGIV and EGV)

118 and two β -glucosidases (BGLI and BGLII) that act in synergy to degrade lignocellulosic
119 materials (Herpoël-Gimbert et al., 2008). Proteomic studies have investigated the secretome
120 and/or intracellular proteins synthesized by filamentous fungi (Peterson and Nevalainen,
121 2012) by combining one-dimensional (1D) or two-dimensional (2D) gel electrophoresis with
122 protein identification by liquid chromatography/ mass spectrometry. This technique allows
123 the analysis of the multicomponent cocktail of cellulolytic enzymes secreted by *T. reesei* in
124 culture media (Herpoël-Gimbert et al., 2008; Jun et al., 2013; Kubicek, 2013), and to
125 investigate the differential protein synthesis at intracellular level (Bianco and Perrotta,
126 2015). The influence of carbon source (Jun et al., 2013; dos Santos Castro et al., 2014;
127 Peciulyte et al., 2014), pH (Adav et al., 2011), light intensity (Stappler et al., 2017) and
128 agitation intensity (Mukatoka et al., 1988; Lejeune and Baron, 1995) on extracellular enzyme
129 secretion has also been studied. However, except for Jun et al., 2013, which compared its
130 intracellular proteome with various carbon sources; and Arvas et al., 2011 that studied the
131 intracellular effects of growth rate and cell density in chemostat culture, the impact of
132 culture conditions on intracellular protein synthesis by *T. reesei* remains poorly investigated.
133 To our knowledge, the impact of fluid dynamic stress (here expressed as $EDCF_{\epsilon_{max}}$) on the
134 synthesis of intracellular proteins by *T. reesei* has never been reported.

135 The objective of this work therefore was to characterize the effects of fluid dynamic
136 stress on the production of both intracellular proteins and extracellular cellulases by
137 *T. reesei*.

138 2. Material and Methods

139 2.1. *Strain, preculture and culture media*

140 The *T. reesei* strain used and the composition of the preculture medium and of the
141 batch-culture medium were fully described previously (Hardy et al., 2017). For the
142 production phase, the medium had the same composition as the batch-culture medium but
143 it was supplemented with 0.83 g.L⁻¹ yeast extract instead of powdered corn steep liquor.

144 A 150 mL preculture was prepared in a 2 L Fernbach flask by mixing 135 mL of
145 preculture medium and 15 mL of a sterile glucose solution at 250 g L⁻¹. The flasks were
146 seeded with 1 mL of conidia to give a seeding rate of 10% and held in a shaker incubator
147 (Multiron II, Infors, Bottmingen, Switzerland) for 72 hours at 30°C and 180 rpm with an orbit
148 of 50 mm before being added into the bioreactor culture.

149 2.2. *Bioreactor cultures using two different fluid dynamic stress conditions*

150 This work is a follow on to that reported in Hardy et al. (2017). In that study, the
151 initial batch production of *T. reesei* was studied at the bench scale in a 3.5 L bioreactor
152 with a working volume of 2.5 L and at commercial scale. At the bench scale, a Rayneri
153 centripetal turbine impeller (VMI-mixing, Montaigu, France) (see Fig 1) was used along
154 with 3 others. All of the changes in process performance brought about by fluid dynamic
155 stress for each impeller were successfully related to changes in $EDCF_{\epsilon_{max}}$. In order to move
156 to continuous culture, a different bioreactor had to be selected and one of a similar size
157 was available which used a Rayneri impeller. Since that impeller had fitted in well with the
158 others in the earlier work, in order to have bench scale data in a similar sized bioreactor to

159 aid comparison between the different aspects of the overall study, the present
160 configuration was chosen.

161 A 3.0 L, dished bottomed, stirred bioreactor (ezControl BioBundle, Applikon Biotechnology,
162 Foster, CA, USA) with a working volume of 1.5 L, diameter $T = 126$ mm with a broth height,
163 H mm such that $H/T = 1$ and without baffles but with sufficient probes inserted to provide a
164 significant baffling effect. The Rayneri centripetal turbine impeller was 0.08 m diameter,
165 height, 0.045 m with $Po = 2.0$ and $Fl = 1.3$. The temperature was controlled at 27 °C, pH at
166 4.8 and dissolved oxygen concentration at 70 % by introducing a blend of air and nitrogen
167 (thereby altering the driving force for mass transfer) through a sparger. The total flow rate
168 was held constant at 0.8 L/min so that neither the dO_2 or flow rate changed during the
169 experiment (Hardy et al., 2017). However, as in earlier work (Herpoël-Gimbert et al., 2008),
170 to control to this dO_2 at the bench scale even with gas blending required a high P/V (Hardy
171 et al., 2017) of at least $6 \text{ kW} \cdot \text{m}^{-3}$, which needed a minimum speed of 800 rpm. Such speeds
172 led to very high $EDCF_{\text{max}}$ compared to the commercial scale, where the circulation time is
173 significantly longer and the specific power was kept as low as possible for economic reasons.

174 Two complete runs, each consisting of 3 parts, were undertaken. In each, there was
175 an initial batch phase during which the fungus was grown at an agitation speed of 800 rpm
176 until a fungal biomass concentration of $\sim 7.9 \pm 0.2 \text{ g} \cdot \text{kg}^{-1}$ was reached. Then, the continuous
177 phase of the run was begun, thereby commencing cellulase production. That time is marked
178 as 'start of continuous feed' on Fig 1 and from then, it was held at 800 rpm for another 150
179 hrs which allowed time for approximately 5 volume changes so that a steady state should
180 have been reached (Macauley-Patrick and Finn, 2008). The concentration of biomass and
181 the production of cellulases also indicated an approximate steady state for 50 hrs. At that
182 point, the speed was increased to 1700 rpm to give a higher fluid dynamic stress and then

183 kept constant with the same feed and discharge rate. This condition was held constant for
184 another approximately 140 hrs, equivalent to approximately 4 volume changes, sufficient to
185 approach another steady state and allow the impact of the change on biomass and
186 intracellular and extracellular proteins to be assessed. The experiment was duplicated and
187 samples were withdrawn at regular intervals for biomass and protein concentration
188 measurements and those taken at the times noted on Fig 1 were used for proteomic
189 analysis.

190 In the batch phase, the bioreactor contained 0.75 L 2N culture medium, 0.3 L water
191 and 0.3 L glucose solution (150 g.L^{-1}) and it was inoculated with 0.15 L preculture to give an
192 initial fungal concentration in the medium of 0.8 g.kg^{-1} . During the whole of the continuous
193 phase, the constant feed and discharge rates of two solutions were lactose (180 g.L^{-1}) at
194 6 mL.h^{-1} and the enriched 2N medium at 39 mL.h^{-1} giving a dilution rate, D (0.03 h^{-1}) which
195 since $D = \mu$, the growth rate, is also 0.03 h^{-1} .

196 **2.3. Determination of concentrations in the culture medium**

197 Biomass was quantified as described previously (Hardy et al., 2017) as was lactose
198 following the method used for glucose. The concentration of the cellulases produced was
199 quantified on filtered broth samples according to the Lowry method, by using the Protein
200 Assay DC_{TM} kit (Biorad, Hercules, CA, USA) and a range of bovine serum albumin (BSA)
201 concentrations from 0 to 1.5 g.L^{-1} as standards (Hardy, 2016). β -glucosidase activity was
202 measured as described by Jourdir et al. (2013). All analyses were performed in duplicate.

203 **2.4. Proteomic analyses**

204 The proteomic analyses of intracellular proteins were carried out in 3 steps: protein
205 extraction, two-dimensional (2D) electrophoresis on sodium dodecyl sulfate polyacrylamide

206 gel (SDS PAGE) and identification of proteins by mass spectrometry coupled to liquid
207 chromatography.

208 The cytoplasmic proteins were first extracted by cell grinding from a biomass cake
209 obtained by filtration as previously described. Initially, 0.2 g of biomass cake was washed
210 and re-suspended as described previously (Wang et al., 2011). The cells were lysed with 0.6
211 g of glass beads (0.3 g of diameter 0.1 mm and 0.3 g of diameter 0.5 mm, Biospec Products,
212 Bartlesville, OK, USA) in a FastPrep FP 120 equipment (Bio 101, Savant Instruments,
213 Holbrook, AZ, USA), for four times with cycles of 30 s at an intensity of 6.5. After grinding
214 the cells, the samples containing solubilized cytoplasmic proteins were centrifuged, purified
215 with 60 U endonuclease (Biorad, Hercules, CA, USA) and precipitated, and their protein
216 concentration was assayed using the colorimetric method of Bradford (1976) using bovine
217 serum albumin as a standard in order to ensure 300 µg of proteins were present (Wang et
218 al., 2011).

219 The separation of the extracted proteins was achieved by successive separation
220 according to their isoelectric point by isoelectric focusing (IEF) and to their molecular weight
221 by SDS-page electrophoresis. All samples from the two conditions were analyzed in triplicate
222 from three different extractions. The cell extracts containing 300 µg of proteins were diluted
223 in 350 µL of extraction buffer [31]. To perform IEF, the diluted samples were loaded onto
224 Immobiline DryStrip gels (pI 4-7, 17 cm, Biorad) that were submitted to electric focusing at
225 20°C on an IEF Cell (Biorad, Hercules, CA, USA) to reach 73,000 Wh for about 24 hours.

226 After equilibration of the DryStrip gels, the second dimension separation was
227 performed in SDS-polyacrylamide gels as described by Wang et al. (2011). Proteome image
228 analysis was carried out with PDQuest 2-D software (Biorad) to compare the proteins
229 density on the gels obtained from different conditions. Spots only present on one gel

230 condition or showing a difference in density greater than a factor of 2 were considered as
231 different between two conditions and retained for identification.

232 The spots corresponding to the differentially synthesized proteins were collected,
233 washed separately with 50 mM ammonium hydrogen carbonate and 50 % acetonitrile and
234 then dried. After digestion with 0.5 μg of trypsin (Promega, Madison, WI) and 50 mM
235 ammonium hydrogen carbonate for 12 h at 37 °C, the supernatant containing peptides were
236 used for protein identification by tandem mass spectrometry coupled to liquid
237 chromatography (LC-MS / MS) using a LTQ-XL mass spectrophotometer (ThermoFinnigan,
238 Waltham, MA, USA) (PAPPSO, Gif-sur-Yvette, France). The sequences were identified using
239 the Joint Genome Institute databases (JGI, Walnut Creek, CA USA).

240 **3. Results and Discussion**

241 **3.1. Estimation of the fluid dynamic stress, $EDCF_{\varepsilon_{max}}$**

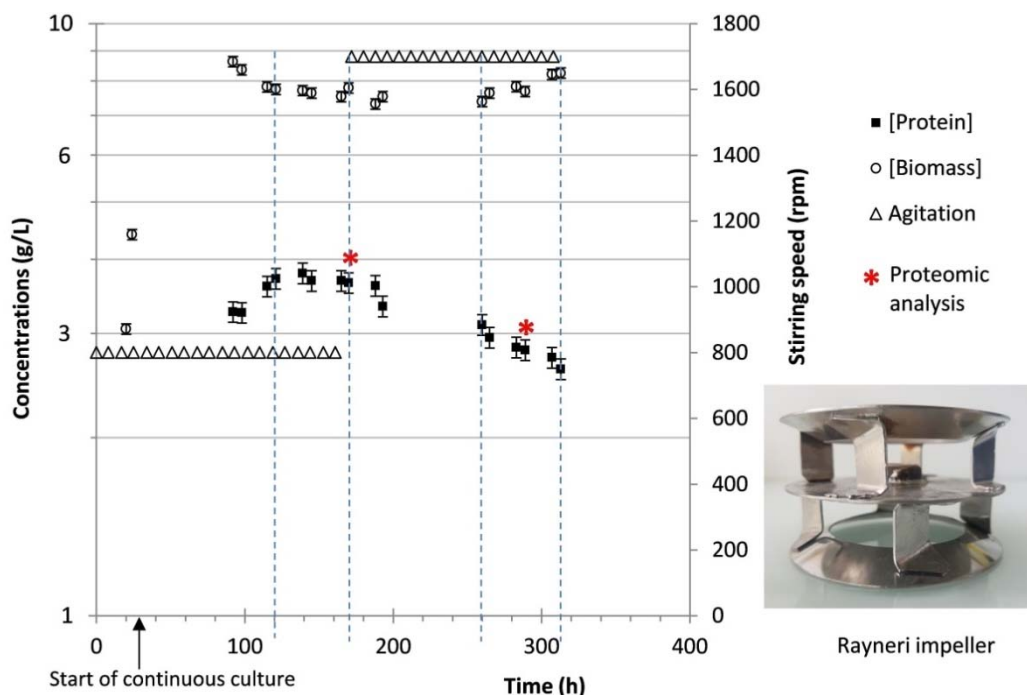
242 In order to estimate ε_{max} (see Section 1), a value of x is required. The values (Grenville
243 et al., 2017) for different impellers range from 12 to 17 but one is not available for the
244 Rayneri impeller, which is a very different shape to others (see Fig 1). However, it
245 produces radial flow as does a Rushton turbine which has an x value of 12 and this
246 value is initially assumed here. Thus $EDCF_{\varepsilon_{max}}$ was 1884 and 38,400 $\text{kW}\cdot\text{m}^{-3}\cdot\text{s}^{-1}$
247 respectively, a little higher than used previously (Hardy et al., 2017) because though
248 similar speeds were used, here the bioreactor volume was smaller.

249 At the commercial scale, multiple impellers were used but the Rushton turbine
250 provided most of the power input (Hardy et al., 2017). Thus, both the Po value and x
251 of the Rushton turbine were chosen for the determination of $EDCF_{\varepsilon_{max}}$ for the
252 commercial scale, which as explained earlier was very much lower at $\sim 6.65 \text{ kW}\cdot\text{m}^{-3}\cdot\text{s}^{-1}$

253 (Hardy et al., 2017). Overall, $EDCF_{\text{emax}}$ was the best correlator of hyphal size, broth
254 rheology and growth rate for all the impellers and across these scales.

255 3.2. Effect of fluid dynamic stress, $EDCF_{\text{emax}}$, on the production of cellulases

256 The details of the runs are given in Section 2.2. Figure 1 shows the biomass and
257 protein concentration throughout the culture whilst Table 1 gives the mean biomass and
258 cellulase concentrations at the first steady state (the lower $EDCF_{\text{emax}}$) and the near-steady
259 state at the higher $EDCF_{\text{emax}}$. Table 1 also gives the value of a range of other process
260 parameters obtained for these two conditions and p values from ANOVA tests for the results
261 for the time periods indicated by the dotted lines on Fig 1. The variables describing the
262 biomass (biomass concentration, specific growth rate, growth yield) were not influenced by
263 the agitation rate (p-values higher than 0.05). The variables that characterize the protein
264 production (protein concentration, specific production rate, production and conversion
265 yields and β -glucosidase activity) were significantly affected by the $EDCF_{\text{emax}}$ value (p-values
266 lower than 0.05).



268 **Figure 1:** Biomass and protein concentrations during continuous culture agitated by a
 269 Rayneri centripetal turbine impeller (embedded image) at initially 800 rpm increasing to
 270 1700 rpm ($EDCF_{\epsilon_{max}}$ 1884 and 38,400 $\text{kW}\cdot\text{m}^{-3}\cdot\text{s}^{-1}$ respectively). Dotted lines indicate time
 271 periods used for ANOVA tests. Error bars represent the standard deviation.

272

273 **Table 1:** Measured values of culture parameters and associated p-values at the two
 274 different speeds and $EDCF_{\epsilon_{max}}$ values

Stirring speed	800 rpm	1700 rpm	p-value
$EDCF_{\epsilon_{max}}$ ($\text{kW}\cdot\text{m}^{-3}\cdot\text{s}^{-1}$)	1884	38400	na
Biomass concentration, X ($\text{g}\cdot\text{kg}^{-1}$)	7.7 ± 0.2	7.6 ± 0.2	0.538
Specific growth rate, μ (h^{-1})	0.028 ± 0.01	0.028 ± 0.03	0.064
Protein concentration, P ($\text{g}\cdot\text{kg}^{-1}$)	3.7 ± 0.1	2.9 ± 0.1	0.001
Specific protein (cellulases) production rate, q_p ($\text{g}\cdot\text{kg}^{-1}\cdot\text{h}^{-1}$)	13.5 ± 0.5	10.3 ± 0.8	0.0002
Specific substrate consumption rate, q_s ($\text{g}\cdot\text{kg}^{-1}\cdot\text{h}^{-1}$)	0.084 ± 0.002	0.077 ± 0.002	0.0001
β -Glucosidase activity (IU/mL)	129.0 ± 1.7	107.9 ± 1.2	0.001
$Y_{X/S}$ ($\text{g}\cdot\text{g}^{-1}$)	0.35 ± 0.02	0.36 ± 0.04	0.471
$Y_{P/S}$ ($\text{g}\cdot\text{g}^{-1}$)	0.17 ± 0.01	0.13 ± 0.01	0.005
$Y_{P/X}$ ($\text{g}\cdot\text{g}^{-1}$)	0.48 ± 0.02	0.37 ± 0.02	0.002

275 *The data presented corresponds to the mean values for each condition (800 and 1700 rpm) for the*
 276 *period shown on Figure 1 and their standard deviations. Legend as in Nomenclature ; na: not*
 277 *applicable.*
 278

279 The specific growth rate remained unchanged since a constant value was imposed by
 280 the constant dilution rate, D . However, constant biomass concentration is globally
 281 determined as cell dry weight. Ideally, the biomass concentration should also be subdivided
 282 into the percentage of active and inactive/damaged cells. However, reliable techniques for
 283 quantitatively measuring the viability of filamentous fungi are not available whether by
 284 fluorescent dyes, because of sampling issues, or by flow cytometry, because of the
 285 filamentous structure of the fungi which tends to block the capillaries. On the other hand,
 286 the constant biomass implies that it should all be active.

287 Table 1 and Figure 1 show that the specific production rate decreased by 24 % and
 288 the protein production yields in relation to sugar and to biomass concentration decreased
 289 by 20 % and 23 % respectively with p values again showing statistical significance. These

290 results agree with previous studies on the effect of fluid dynamic stress on secondary
291 metabolites production by filamentous fungus in stirred bioreactors. Jüsten et al. (1998)
292 observed increase in $EDCF$ with different impellers decreased penicillin production during
293 fed-batch fermentations of *P. chrysogenum*. Lejeune and Baron (1995) and Mukataka et al.
294 (1988) found a lower production of cellulases at higher speeds with *T. reesei* cultures but did
295 not analyze the impact of different impellers or quantify hydrodynamic stress beyond
296 agitator speed. Reese and Ryu (1980) determined the effect of 'shear' on the stability of a
297 crude cellulase preparation of *T. reesei* and found that it caused deactivation of the enzyme
298 exoglucanase cellobiohydrolase (CBH), which slowed down cellulose digestion in a cellulosic
299 biomass hydrolysis. Ganesh et al. (2000) observed similar inactivation with increasing speed
300 in stirred reactors. These studies confirm that higher fluid dynamic stresses lead to a
301 decrease in cellulases production by *T. reesei* and to a deactivation of components of its
302 cellulolytic cocktail.

303 **3.3. Effect of higher fluid dynamic stress on the synthesis of intracellular proteins**

304 Scanned pictures of the two SDS-PAGE gels from proteomic analysis of cells are given
305 in Figure 1 (Supplementary Material). The gels indicate intracellular proteins that were
306 differently synthesized at the two $EDCF_{\epsilon_{max}}$ values of 1884 and 38,400 $\text{kW}\cdot\text{m}^{-3}\cdot\text{s}^{-1}$
307 respectively. Image analysis of these gels allowed these proteins to be collected and
308 identified. In total, 30 spots, which corresponded to 24 different proteins, had their
309 synthesis modified as $EDCF_{\epsilon_{max}}$ increased. They were identified by tandem mass
310 spectrometry coupled with liquid chromatography (LC-MS/MS) and compared with *in silico*
311 data from sequence libraries as described in Section 2. At the higher $EDCF_{\epsilon_{max}}$, six proteins
312 were newly-synthesized (NW1 to NW6 in Table 2); six proteins were increasingly-

313 synthesized (up-regulated) by times 2 or more (UP1 to UP6, Table 3); and 18 proteins were
314 under-synthesized (down-regulated) by times 2 or more (UN1 to UN18, Table 4).

315 An analysis of Table 2 shows the increase in $EDCF_{\epsilon_{max}}$ only produced five new
316 proteins, as two of the 6 spots are isoforms of the same protein. Of the others, three assist
317 in protein quality control (including one chaperonin and two ubiquitin dependent
318 proteasomes) and are recognized as stress proteins. From Table 3, three up-synthesized
319 proteins are involved in the central carbon metabolism as they are related to
320 oxidoreductase activity (dihydrolipoyl dehydrogenase and FAD/NAD(P) domain-containing
321 protein) and Acetyl CoA biosynthesis (acetate kinase). The four others are involved in carbon
322 metabolism (adenosylhomocysteinase), proteolysis (glutamate carboxypeptidase) and GDP-
323 mannose biosynthesis (phosphomannomutase). Finally, of the under-synthesized proteins
324 (Table 4), there are a number of isoforms and only 12 different ones are identified from 18
325 spots of which four relate to cellulolytic (glucosidases, endoglucanase and
326 cellobiohydrolases) and hemicellulolytic (xyloglucanases) activities. Of the eight others, one
327 involved putrescine biosynthesis (putative agmatine deiminase), two to transferase activity
328 (transketolase and uracil phosphoribosyl transferase) plus one isomerase (UDP-glucose-4-
329 epimerase), one kinase (diphosphomevalonate decarboxylase), one oxidoreductase
330 (NAD(P)H-dependent-D-xylose reductase), one involved in Ca^{2+} homeostasis (SGL domain-
331 containing protein) and one implicated in proteolysis (Zn-dependent exopeptidases).
332 Overall, two groups of proteins can be highlighted: under the higher $EDCF_{\epsilon_{max}}$, stress
333 proteins were over-synthesized (up-regulated) and cellulases were under-synthesized (down
334 –regulated).

335

Table 2: Proteins newly-synthesized by the increase from 800 to 1700 rpm ($EDCF_{\epsilon_{max}}$ 1884 and 38,400 kW.m⁻³.s⁻¹ respectively)

Spot	Protein ID*	Protein description	MW (KDa) in the 2D gel	IP in the 2D gel	Coverage** (%)	Functional category
NW1	135423	Chaperonin HSP60	63.1	5.25	75	Chaperone molecular family
NW2	26797	20S proteasome subunit alpha type (homologs PSMA4 / PRE9)	26.2	6.12	73	Threonine endopeptidase activity - Ubiquitin-dependent protein
NW3	99350	20S proteasome alpha type (homologs PSMA6 / SCL1)	26.3	6.30	73	
NW4	80225	Uroporphyrinogen decarboxylase	39.2	5.99	71	Porphyrin biosynthesis
NW5 & NW6***	39524	Malate dehydrogenase	35.5	5.92	37	Oxidoreductase activity - Carbohydrate metabolism
			35.5	6.22	49	

336

*MW: molecular weight; IP: isoelectric pH; *Protein ID were obtained from JGI database; **Coverage corresponds to the percentage of the protein sequence*

337

*covered by identified peptides; ***Spots that correspond to isoforms of the same protein*

338

339

340

Table 3: Proteins over-synthesized from the increase from 800 to 1700 rpm ($EDCF_{emax}$ 1884 and 38,400 $\text{kW}\cdot\text{m}^{-3}\cdot\text{s}^{-1}$ respectively)

Spot	Protein ID*	Protein description	MW (KDa) in the 2D gel	IP in the 2D gel	Coverage** (%)	Log2 fold change	Functional category
UP1	78299	Dihydrolipoyl dehydrogenase	55.3	6.47	77	1.9	Oxidoreductase activity - Cell redox homeostasis
UP2	25190	FAD/NAD(P)-binding domain-containing protein	59.5	6.07	78	1.4	
UP3	97186	Phosphomannomutase	28.1	5.38	71	1.3	GDP-mannose biosynthetic process
UP4	137356	Glutamate carboxypeptidase	57.8	5.69	82	2.5	Proteolysis
UP5	99242	Acetate kinase	46.6	6.49	81	1.3	Acetyl-CoA biosynthesis
UP6	142425	Adenosylhomocysteinase	46.0	6.22	68	1.5	Nucleic acid and amino-acid metabolism

341

*MW: molecular weight; IP: isoelectric pH; *Protein ID were obtained from JGI database; **Coverage corresponds to the percentage of the protein sequence*

342

covered by identified peptides

343

344

Table 4: Proteins under-synthesized by the increase from 800 rpm to 1700 rpm ($EDCF_{emax}$ 1884 and 38,400 kW.m⁻³.s⁻¹ respectively)

Spot	Protein ID*	Protein description	MW (KDa) in the 2D gel	IP in the 2D gel	Coverage** (%)	Log2 fold change	Functional category
UN1	122470	Exoglucanase II (1,4- β -cellobiohydrolase)	63.5	5.22	67	-2.3	
UN2	124438	Endo- β -1,4-glucanase	22.8	5.81	71	-2.3	
UN3 to UN7***	136547	β -D-glucoside glucohydrolase I	94.8	5.98	66	-1.5	Hydrolase activity – Cellulases
			91.8	6.15	65	-1.5	
			74.9	6.15	67	-2.8	
			74.5	6.34	69	-2.6	
			75.7	6.49	71	-2.8	
UN8 & UN9***	111943	Xyloglucanase	96.5	4.97	61	-2.4	Hydrolase activity – Hemicellulase
			92.1	4.87	63	-1.5	
UN10	108605	Uracil phosphoribosyl transferase	25.4	5.82	85	-1.2	Transferase activity - Nucleoside metabolism
UN11	111063	Peptide hydrolase	67.5	4.60	58	-2.3	Proteolysis
UN12 & UN13***	102903	Putative agmatine deiminase	47.0	4.55	84	-1.5	Putrescine biosynthesis
			46.8	4.65	40	-2.6	

UN14	99640	SMP30/gluconolactonase / LRE-like protein	33.7	5.12	75	-1.2	Ca ²⁺ homeostasis and signal transduction
UN15	101957	Diphosphomevalonate decarboxylase	36.0	5.63	45	-1.1	Kinase activity - ATP binding - Phosphorylation
UN16	137982	UDP-glucose 4-epimerase	37.0	6.15	39	-1.3	Coenzyme binding - Isomerase activity - Cellular metabolism
UN17	94809	NAD(P)H-dependent D- xylose reductase	24.4	5.08	53	-1.6	Oxidoreductase activity
UN18	110941	Transketolase	74.7	6.39	72	-2.9	Transferase activity – Metal ion binding - Carbohydrate metabolism

346 *MW: molecular weight; IP: isoelectric pH; *Protein ID were obtained from JGI database; ** Coverage corresponds to the percentage of the protein sequence*

347 *covered by identified peptides; ***Spots that correspond to isoforms of the same protein*

348 3.3.1. *Effect of higher fluid dynamic stress on the synthesis of stress proteins*

349 It is known that environmental stresses cause protein denaturation by aggregation
350 and misfolding leading to loss of biological functions and cell apoptosis (Roller and Maddalo,
351 2013; Tiwari et al., 2015). Table 2 and Figure 1 (Supplementary Material) show the higher
352 speed ($EDCF_{\epsilon_{max}}$) produces the chaperonin protein HSP60 and the ubiquitin-proteasome
353 system which are known to reduce cell damage by acting on post-translational processes
354 (Tiwari et al., 2015), correcting protein folding, helping refolding and stabilizing them under
355 stress (Pickart, 1999). Specifically, HSP60 has a crucial role in synthesis, transportation,
356 folding and degradation of proteins (Chen et al., 1999) and its over-expression under heat
357 (Raggam et al., 2011; Tiwari et al., 2015) and heavy metal (Enjalbert et al., 2006) stress has
358 been reported in fungal pathogens. Kashyap et al., 2016 observed its expression under
359 saline stress in halotolerant fungus *P. clavariiformis*. The ubiquitin-proteasome system
360 performs a similar function (Shang and Taylor, 2011; Kashyap et al. (2016) with various
361 fungi; for example, nitrogen deprivation (Shang and Taylor, 2011), heat shock (Staszczak,
362 2008) and exposure to cadmium (Goller et al., 1998).

363 The present study clearly shows for the first time that the cells response to higher
364 fluid dynamic stress is similar to that with other environmental stresses in order to protect
365 themselves against irreversible damage.

366 3.3.2. *Effect of fluid dynamic stress on the synthesis of cellulases*

367 Figure 1 (Supplementary Material) and Table 4 show that at the higher $EDCF_{\epsilon_{max}}$, the
368 synthesis of four intracellular cellulases decreased: glucosidases (β -D-glucoside
369 glucohydrolase I), endoglucanases (endo-1,4- β -glucanases), cellobiohydrolases (exo-1,4- β -
370 glucanases) and xyloglucanases. The first three make up the *T. reesei* cellulolytic cocktail

371 (Jourdier et al., 2013). Cellobiohydrolases attack the cellulose chains from the ends,
372 releasing cellobiose molecules. Endoglucanases hydrolyze cellulose chains randomly,
373 generate new ends accessible to cellobiohydrolases. β -glucosidase has the role of
374 hydrolyzing into glucose the cellobiose released by the action of endoglucanases and
375 cellobiohydrolases. This synergistic action is essential for hydrolysis of lignocellulosic
376 biomass by the fungus (Kumar et al., 2008) as are xyloglucanases (Herpoël-Gimbert et al.,
377 2008) for improving hydrolysis efficiency as the hemicellulolytic activity of this enzyme
378 increases the surface area (Benkő et al., 2008).

379 The fact that the synthesis of cytoplasmic cellulases is negatively affected by higher
380 fluid dynamic stress is strongly linked to the reduction of extracellular cellulases (Figure 1
381 and Table 1). This result indicates that the profile of extracellular proteins is directly linked
382 to the synthesis of intracellular proteins, as demonstrated above from the proteomic
383 analysis. This finding is original because, although some authors have reported the negative
384 effects of 'shear' stress on the secretion of cellulases by *T. reesei* (Mukatana et al., 1988;
385 Lejeune and Baron, 1995), the literature has not made any connection with the effect of
386 fluid dynamic stress on the intracellular synthesis of cellulases.

387 **3.4. Effect of scale on the production of cellulases**

388 For this study in chemostat culture, $EDCF_{\text{max}}$ was 1884 kW.m⁻³.s⁻¹ and 38400 kW.m⁻
389 ³.s⁻¹ and the proteomic analysis showed that, as a result, a change took place at the
390 intracellular level to protect the cells and partially maintain the production of cellulases. As
391 a result of this protective action, though $EDCF_{\text{max}}$ increased substantially, the fall in cellulase
392 production was relatively small, from 13.5 to 10.3 g.kg⁻¹. h⁻¹.

393 In the batch cultures previously reported (Hardy et al., 2017) (i.e. during the growth
394 phase of the fermentation), $EDCF_{\epsilon_{max}}$ was a little smaller at the bench scale than here
395 because a larger bench scale bioreactor was used. As usual, it was also much lower than at
396 the commercial scale ($6.65 \text{ kW}\cdot\text{m}^{-3}\cdot\text{s}^{-1}$) for the reasons given earlier (Hardy et al., 2017) and
397 in Section 3.1. The lower $EDCF_{\epsilon_{max}}$ was mirrored by increases in the growth rate, the
398 viscosity of the broth and the size of the fungi.

399 At the commercial scale (Hardy et al., 2017), since the aim was to produce as much
400 cellulase as possible, fed batch culture was used for the production phase to give a q_p of 17
401 $\text{g}\cdot\text{kg}^{-1}\cdot\text{h}^{-1}$. In bench scale work (Hardy, 2016) related to this continuous culture study and the
402 earlier batch study (Hardy et al., 2017), two fed batch cultures were also undertaken. These
403 fed-batch studies were done in the same 3.5 L bioreactor as used by Hardy et al. (2017) with
404 the Rayneri centripetal impeller at 1000 rpm to give an $EDCF_{\epsilon_{max}}$ of $2760 \text{ kW}\cdot\text{m}^{-3}\cdot\text{s}^{-1}$. The
405 biomass concentration was controlled to 3.5 g/kg or 12 g/kg but the impact on the
406 production of cellulases was not statistically significant ($q_p = 11.9 \pm 3.3 \text{ g}\cdot\text{kg}^{-1}\cdot\text{h}^{-1}$). Clearly,
407 the scatter was large (Hardy, 2016). It is interesting to compare the small change in q_p for
408 cellulase production with the very different $EDCF_{\epsilon_{max}}$ values in the continuous culture
409 conditions reported here and those arising in fed-batch at the two very different scales. It is
410 also convenient to assess whether the choice of $x = 12$ for the Rayneri impeller is an
411 appropriate one.

412 Hardy et al. (2017) showed that in batch culture, the growth rate μ is linked with
413 $EDCF_{\epsilon_{max}}$ and under the conditions studied, the growth rate was well described by the
414 empirical function, Eq 1 for all the impellers tested at the bench scale and for the data
415 obtained at the commercial scale:

$$\mu = A \cdot \ln(EDCF_{\varepsilon_{max}})_{batch} + B \quad (1)$$

416 In order to investigate the effect of $EDCF_{\varepsilon_{max}}$ on the specific production rate q_p , a similar
 417 analysis is proposed. However, given the low number of experiments performed, it is not
 418 possible to validate the function proposed by Hardy et al. (2017) or indeed any other
 419 function. Given this situation, it has been assumed as a working hypothesis, that a similar
 420 function of $EDCF_{\varepsilon_{max}}$ is usable with other constants A and B. Thus,

$$q_{p_{cont}} = A \cdot \ln(EDCF_{\varepsilon_{max}})_{cont} + B \quad (2)$$

421 Based on this hypothesis, the results of the present work are used to fit constants to
 422 Eq 2 and then used for scale-up consideration. Using the q_p values obtained in the present
 423 work at the two $EDCF_{\varepsilon_{max}}$ gives A = -1.05 and B = 21.4. Eq 2 can now applied to the fed-batch
 424 case at the bench (subscript fb1) and commercial scale (subscript fb2) to give the empirical
 425 Eq 3:

$$q_{p_{fb2}} = q_{p_{fb1}} - A \cdot \ln \left(EDCF_{\varepsilon_{max_{fb1}}} / EDCF_{\varepsilon_{max_{fb2}}} \right) \quad (3)$$

426 If it is assumed that though different fermentation methods (fed-batch and continuous) give
 427 different product yields, the impact of fluid dynamic stress is the same for the particular
 428 organism, then the specific production rate at commercial scale can be obtained by Eq 4:

$$q_{p_{fb2}} = 11.9 + 1.05 \cdot \ln(2760/6.65) = 18.3 \quad (4)$$

429 This predicted value of q_p (18.3 g.kg⁻¹.h⁻¹) at the commercial scale is similar to the actual one
 430 (17 g.kg⁻¹.h⁻¹), especially considering the large difference in the scales used for these two
 431 fed-batch runs and that other factors can come into play at the commercial scale such as
 432 increased levels of inhomogeneity due to the greater mixing time and pCO₂ and dO₂ due to
 433 the static head. Nevertheless, it is clear that more data are required to confirm this
 434 relationship.

435 Table 5 summarizes the different culture conditions, scales, process parameters,
 436 $EDCF_{\epsilon_{max}}$ and results obtained in the whole of this wide ranging study.

437 **Table 5.** Comparison of the three different culture conditions and results obtained in this
 438 overall wide ranging study.

Source	Culture Conditions	Bioreact or Scale	Process Parameters	$EDCF_{\epsilon_{max}}$ ($\text{kW}\cdot\text{m}^{-3}\cdot\text{s}^{-1}$)	Results
Hardy (2016)	Fed batch	3.5 L and ~100 m ³	q_p	2760 and 6.65	q_p : 0.012 and 0.017 g.kg ⁻¹ .h ⁻¹
Hardy et al., (2017)	Batch	3.5 L and ~100 m ³	Rheology, biomass and morphology Y	24000 to 6.6	$Y = A \cdot \ln(EDCF_{\epsilon_{max}}) + B$
This work	Continuous	3.0 L	q_p	38400 and 1880	q_p : 0.010 and 0.014 g.kg ⁻¹ .h ⁻¹

439
 440 The question regarding the impact of the value of x (the ratio of impeller diameter to
 441 trailing vortex diameter) chosen for the Rayneri impeller can also be addressed in relation to
 442 this type of analysis. Grenville et al. (2017) give a range of x values from 12 to 17 with 12
 443 being the value for the Rushton turbine and chosen for the Rayneri because, though very
 444 different from most impellers, they are both radial flow. If the other extreme, $x = 17$, is
 445 chosen to test the range of possible impacts on this analysis, then the $EDCF_{\epsilon_{max}}$ values of the
 446 continuous cultures reported in Table 1 are multiplied by 17/12, the B parameter of Eq.1
 447 becomes 21.9 instead of 21.4, and the A parameter remains unchanged. Applying the same
 448 x value of 17 for the bench scale fed batch run, $EDCF_{\epsilon_{max}}$ becomes 3910 $\text{kW}\cdot\text{m}^{-3}\cdot\text{s}^{-1}$. If this
 449 value is used in Eq 3 then, since $EDCF_{\epsilon_{max}}$ for the large scale where the Rushton turbine
 450 dominates remains the same, the predicted value of q_p for the commercial scale becomes
 451 18.6 g.kg⁻¹.h⁻¹. In this case, the choice of x clearly is not a significant factor in the analysis of
 452 the impact of fluid dynamic stress on the production of cellulases. Therefore given the

453 similarity in flow pattern between the Rayneri impeller and the Rushton turbine, $x = 12$
454 remains the value of choice.

455 Overall, it can be concluded that not only can the use of the $EDCF_{\epsilon_{max}}$ function
456 enable bench scale data to predict hyphal size, broth rheology and growth rate at the
457 commercial scale (Hardy et al., 2017), it also seems to be a promising tool in aiding scale-up
458 in relation to predicting the production of cellulases. Indeed, the production of cellulases at
459 the commercial scale should not be compromised by fluid dynamic stresses. More
460 importantly, the agitation intensity chosen should be based on ensuring it is sufficient to
461 meet the demands of oxygen mass transfer and carbon dioxide stripping along with an
462 adequate blending strategy, including sub-surface addition of nutrients and pH control
463 chemicals (Amanullah et al., 2004). In addition, economic considerations must be taken into
464 account.

465 **4. Conclusion**

466 *T. reesei* was cultivated in continuous cultures at two $EDCF_{\epsilon_{max}}$ values, the lower one
467 ($1884 \text{ kW}\cdot\text{m}^{-3}\cdot\text{s}^{-1}$) until a steady state was reached and the higher ($38400 \text{ kW}\cdot\text{m}^{-3}\cdot\text{s}^{-1}$) until a
468 near-steady state, sufficient to show a significant fall in protein production linked to
469 measureable changes in intracellular proteins. This method of defining fluid dynamic stress
470 has already been successful in correlating its impact in the batch growth phase of *T. Reesei*
471 at the bench and commercial scale (Hardy et al., 2017). Here, the use of $EDCF_{\epsilon_{max}}$ provided a
472 link between this bench scale continuous culture study with that batch work (Hardy et al.,
473 2017) and also related fed-batch culture to produce cellulases at the bench (Hardy, 2016)
474 and commercial scale ($\sim 100 \text{ m}^3$) (Hardy et al., 2017). It is worthy of note, that a recent

475 extensive review of scale-up methods concluded that the *EDCF* function was the best way of
476 defining agitation intensity in bioprocessing (Böhm et al., 2019).

477 At the higher $EDCF_{\epsilon_{max}}$ at the bench scale, the concentration of the cellulases in the
478 medium as well as the production yield and the specific production rate decreased by 21 %,
479 20 % and 24 % respectively. A proteomic analysis provided further insight that helped to
480 explain these observations. Firstly, at the higher $EDCF_{\epsilon_{max}}$, the intracellular synthesis of all
481 enzymes involved in cellulosic activity was decreased. On the other hand, stress proteins
482 such as the HSP60 chaperone protein and the ubiquitin-proteasome system whose role is to
483 protect the cells from the effects of fluid dynamic stress appeared. These findings
484 demonstrate that at higher fluid dynamic stress, the fungus adapts itself by triggering
485 protection and damage repair mechanisms at the intracellular level and by favoring its
486 central metabolism to the detriment of other less essential functions, the combination of
487 the two explaining the small decrease of cellulase biosynthesis even at much higher
488 $EDCF_{\epsilon_{max}}$.

489 The higher extracellular cellulase production (q_p) at the lower $EDCF_{\epsilon_{max}}$ in continuous
490 culture compared to that at the higher $EDCF_{\epsilon_{max}}$ is quantitatively similar to the increase in q_p
491 during fed-batch fermentation at the commercial scale compared to that at the bench scale.
492 Perhaps more importantly for the commercial aim of producing cellulases, the sensitivity to
493 fluid dynamic stress is relatively small as the proteomic analysis explains.

494

495 **Acknowledgements**

496 The authors acknowledge the Plateforme d'Analyse Protéomique de Paris Sud Ouest
 497 (PAPPSO, Gif-sur-Yvette, France) for help in identifying the proteins. Funding: This work was
 498 supported by the Agence de l'Environnement et de la Maîtrise de l'Energie (ADEME, Angers,
 499 France) by providing financial support for the PhD study of Nicolas Hardy [number
 500 2016SACLA017].

501

502 **Nomenclature**

D	dilution rate (h^{-1}) or impeller diameter (m)
dO_2	dissolved oxygen concentration (% of saturation value at ambient pressure)
$EDCF_{\epsilon_{max}}$	EDCF based on the maximum specific energy dissipation rate ($\text{W}\cdot\text{m}^{-3}\cdot\text{s}^{-1}$)
Fl	flow number of the impeller (dimensionless)
IP	isoelectric pH (dimensionless)
MW	molar weight (kDa)
N	rotation speed ($\text{rev}\cdot\text{s}^{-1}$)
P	protein concentration ($\text{g}\cdot\text{kg}^{-1}$) or power input from impeller (W)
Po	power number of the impeller (dimensionless)
q_p	specific protein production rate ($\text{g}\cdot\text{kg}^{-1}\cdot\text{h}^{-1}$)
q_s	specific substrate consumption rate ($\text{g}\cdot\text{kg}^{-1}\cdot\text{h}^{-1}$)
t	time (s in ϵ_{max} and $EDCF_{\epsilon_{max}}$ or h in Table 1)
t_c	circulation time (s^{-1})
V	volume of broth (L in Table 1 and m^3 in P/V)
x	ratio of impeller diameter to trailing vortex diameter
X	biomass concentration ($\text{g}\cdot\text{kg}^{-1}$)
$Y_{X/S}$	biomass yield in relation to substrate ($\text{g}\cdot\text{g}^{-1}$)
$Y_{P/S}$	protein yield in relation to substrate ($\text{g}\cdot\text{g}^{-1}$)
$Y_{P/X}$	protein yield in relation to biomass ($\text{g}\cdot\text{g}^{-1}$)
ϵ_{max}	maximum local specific energy dissipation rate ($\text{W}\cdot\text{m}^{-3}$)
ρ	density ($\text{kg}\cdot\text{m}^{-3}$)
μ	specific growth rate (h^{-1} or $\text{g}\cdot\text{g}^{-1}\cdot\text{h}^{-1}$)
Subscripts	
fb	fed-batch
$cont$	continuous culture

503

504 **References**

- 505 Adav, S.S., Ravindran, A., Chao, L.T., Tan, L., Singh, S., Sze, S.K., 2011. Proteomic analysis of pH and
506 strains dependent protein secretion of *Trichoderma reesei*. J. Proteome Res. 10, 4579–4596.
507 10.1021/pr200416t.
- 508 Albaek, M.O., Gernaey, K.V., Hansen, M.S., Stocks, S.M., 2012. Evaluation of the energy efficiency of
509 enzyme fermentation by mechanistic modeling. Biotechnol. Bioeng. 109 (4), 950–961.
510 10.1002/bit.24364.
- 511 Amanullah, A., Buckland, B., Nienow, A.W., 2004. Mixing in the fermentation and cell culture
512 industries, in: Paul, E., Atiemo-Obeng, V., Kresta, S. (Eds.), Handbook of Industrial Mixing: Science
513 and Practice. John Wiley & Sons, Inc., Hoboken N.J., pp. 1071–1170.
- 514 Amanullah, A., Christensen, L.H., Hansen, K., Nienow, A.W., Thomas, C.R., 2002. Dependence of
515 morphology on agitation intensity in fed-batch cultures of *Aspergillus oryzae* and its implications
516 for recombinant protein production. Biotechnol. Bioeng. 77 (7), 815–826.
- 517 Arvas, M., Pakula, T., Smit, B., Rautio, J., Koivistoinen, H., Jouhten, P., Lindfors, E., Wiebe, M.,
518 Penttilä, M., Saloheimo, M., 2011. Correlation of gene expression and protein production rate - a
519 system wide study. BMC Genom. 12 (616), 1–25.
- 520 Benkő, Z., Siika-aho, M., Viikari, L., Réczey, K., 2008. Evaluation of the role of xyloglucanase in the
521 enzymatic hydrolysis of lignocellulosic substrates. Enzyme Microb. Technol. 43, 109–114.
522 10.1016/j.enzmictec.2008.03.005.
- 523 Bianco, L., Perrotta, G., 2015. Methodologies and perspectives of proteomics applied to filamentous
524 fungi: From sample preparation to secretome analysis. Int. J. Mol. Sci. 16, 5803–5829.
525 10.3390/ijms16035803.
- 526 Böhm, L., Hohl, L., Bliatsiou, C., Kraume, M., 2019. Multiphase stirred tank bioreactors – New
527 geometrical concepts and scale-up approaches. Chem. Ing. Tech. 91 (12), 1724–1746.
528 10.1002/cite.201900165.
- 529 Bradford, M.M., 1976. A rapid and sensitive method for the quantitation of microgram quantities of
530 protein utilizing the principle of protein-dye binding. Analytical Biochemistry 72, 248–254.
- 531 Chen, W., Syldath, U., Bellmann, K., Burkart, V., Kolb, H., 1999. Human 60-kDa heat-shock protein: A
532 danger signal to the innate immune system. J. Immunol. Res. 162, 3212–3219.
- 533 dos Santos Castro, L., Pedersoli, W.R., Antoniêto, A. C. C., Steindorff, A.S., Silva-Rocha, R., Martinez-
534 Rossi, N., Rossi, A., Brown, N.A., Goldman, G.H., Faça, V.M., Persinoti, G.F., Silva, R.N., 2014.
535 Comparative metabolism of cellulose, sophorose and glucose in *Trichoderma reesei* using high-
536 throughput genomic and proteomic analyses. Biotechnol. Biofuels 7 (41).
- 537 Enjalbert, B., Smith, D.A., Cornell, M.J., Alam, I., j, Nicholls, S., Brown, A.J.P., Quinn, J., 2006. Role of
538 the Hog1 stress-activated protein kinase in the global transcriptional response to stress in the
539 fungal pathogen *Candida albicans*. Mol. Biol. Cell. 17, 1018–1032.
- 540 Fernández-Alejandre, K.I., Flores, N., Tinoco-Valencia, R., Caro, M., Flores, C., Galindo, E., Serrano-
541 Carreón, L., 2016. Diffusional and transcriptional mechanisms involved in laccases production by
542 *Pleurotus ostreatus* CP50. Journal of biotechnology 223, 42–49. 10.1016/j.jbiotec.2016.02.029.
- 543 Ferreira, N.L., Margeot, A., Blanquet, S., Berrin, J.-G., 2014. Use of cellulases from *Trichoderma reesei*
544 in the twenty-first century — Part I: Current industrial uses and future applications in the
545 production of second ethanol generation, in: Gupta, V.K., Schmoll, M., Herrera-Estrella, A.,
546 Upadhyay, R.S., Druzhinina, I., Tuhoy, M.G. (Eds.), Biotechnology and Biology of *Trichoderma*.
547 Elsevier, pp. 245–261.

548 Gabelle, J.-C., Jourdier, E., Licht, R.B., Ben Chaabane, F., Henaut, I., Morchain, J., Augier, F., 2012.
549 Impact of rheology on the mass transfer coefficient during the growth phase of *Trichoderma*
550 *reesei* in stirred bioreactors. Chem. Eng. Sci. 75, 408–417. 10.1016/j.ces.2012.03.053.

551 Ganesh, K., Joshi, J.B., Sawant, S.B., 2000. Cellulase deactivation in a stirred reactor. Biochem. Eng. J.
552 4, 137–141.

553 Goller, S.P., Gorfer, M., Kubicek, C.P., 1998. *Trichoderma reesei* prs12 encodes a stress and unfolded-
554 protein-response-inducible regulatory subunit of the fungal 26S proteasome. Current Genetics
555 33, 284–290. 10.1007/s002940050338.

556 Grenville, R.K., Giacomelli, J.J., Padron, G., Brown, D.A.R., 2017. Mixing: Impeller performance in
557 stirred tanks: Characterizing mixer impellers on the basis of power, flow, shear and efficiency.
558 Chem. Eng. 124 (8), 42–51.

559 Hardy, N., 2016. Identification des critères d’extrapolation du procédé de production de cellulases
560 par *Trichoderma reesei* en utilisant l’approche « scale-down ». Doctoral dissertation, France.

561 Hardy, N., Augier, F., Nienow, A.W., Béal, C., Ben Chaabane, F., 2017. Scale-up agitation criteria for
562 *Trichoderma reesei* fermentation. Chem. Eng. Sci. 172, 158–168. 10.1016/j.ces.2017.06.034.

563 Hardy, N., Henaut, I., Augier, F., Béal, C., Ben Chaabane, F., 2015. Rhéologie des champignons
564 filamenteux: Un outil pour la compréhension d’un procédé de production de biocatalyseurs
565 utilisés pour la production de bioéthanol. Rhéologie 27, 43–48.

566 Herpoël-Gimbert, I., Margeot, A., Dolla, A., Jan, G., Mollé, D., Lignon, S., Mathis, H., Sigoillot, J.-C.,
567 Monot, F., Asther, M., 2008. Comparative secretome analyses of two *Trichoderma reesei* RUT-
568 C30 and CL847 hypersecretory strains. Biotechnol. Biofuels 1 (18). 10.1186/1754-6834-1-18.

569 Jourdier, E., Cohen, C., Poughon, L., Larroche, C., Monot, F., Ben Chaabane, F., 2013. Cellulase
570 activity mapping of *Trichoderma reesei* cultivated in sugar mixtures under fed-batch conditions.
571 Biotechnol. Biofuels 6 (79). 10.1186/1754-6834-6-79.

572 Jun, H., Guangye, H., Daiwen, C., 2013. Insights into enzyme secretion by filamentous fungi:
573 Comparative proteome analysis of *Trichoderma reesei* grown on different carbon sources. J.
574 Proteom. 89, 191–201. 10.1016/j.jprot.2013.06.014.

575 Jüsten, P., Paul, G.C., Nienow, A.W., Thomas, C.R., 1996. Dependence of mycelial morphology on
576 impeller type and agitation intensity. Biotechnol. Bioeng. 52, 672–684.

577 Jüsten, P., Paul, G.C., Nienow, A.W., Thomas, C.R., 1998. Dependence of *Penicillium chrysogenum*
578 growth, morphology, vacuolation, and productivity in fed-batch fermentations on impeller type
579 and agitation intensity. Biotechnol. Bioeng. 59 (6), 762–775.

580 Kashyap, P.L., Rai, A., Singh, R., Chakdar, H., Kumar, S., Srivastava, A.K., 2016. Deciphering the salinity
581 adaptation mechanism in *Penicillium clavariiformis* AP, a rare salt tolerant fungus from
582 mangrove. J. Basic Microbiol. 56, 779–791. 10.1002/jobm.201500552.

583 Kubicek, C.P., 2013. Systems biological approaches towards understanding cellulase production by
584 *Trichoderma reesei*. J. Biotechnol. 163, 133–142. 10.1016/j.jbiotec.2012.05.020.

585 Kumar, R., Singh, S., Singh, O.V., 2008. Bioconversion of lignocellulosic biomass: biochemical and
586 molecular perspectives. Journal of Industrial Microbiology and Biotechnology 35, 377–391.
587 10.1007/s10295-008-0327-8.

588 Lara, A., Galindo, E., Ramírez, O., Palomares, L., 2006. Living with heterogeneities in bioreactors:
589 Understanding the effects of environmental gradients on cells. Mol. Biol. 34, 355–382.
590 10.1385/MB:34:3:355.

591 Lejeune, R., Baron, G.V., 1995. Effect of agitation on growth and enzyme production of *Trichoderma*
592 *reesei* in batch fermentation. Appl. Microbiol. Biotechnol. 43, 249–258.

593 Macauley-Patrick, S., Finn, B., 2008. Modes of Fermenter Operation, in: Mc Neil, B., Harvey, M.L.
594 (Eds.), Practical fermentation technology. John Wiley & Sons Ltd, Chichester,, pp. 69–95.

595 Marten, M., Velkvska, S., Khan, S., Ollis, D., 1996. Rheological, mass transfer, and mixing
596 characterization of cellulase-producing *Trichoderma reesei* suspensions. *Biotechnol. Prog.* 12 (5),
597 602–611.

598 Morales, M., Quintero, J., Conejeros, R., Aroca, G., 2015. Life cycle assessment of lignocellulosic
599 bioethanol: Environmental impacts and energy balance. *Renew. Sustain. Energy Rev.* 42, 1349–
600 1361. 10.1016/j.rser.2014.10.097.

601 Mukataka, S., Kobayashi, N., Sato, S., Takahashi, J., 1988. Variation in cellulase-constituting
602 components from *Trichoderma reesei* with agitation intensity. *Biotechnol. Bioeng.* 32, 760–763.
603 10.1002/bit.260320606.

604 Peciulyte, A., Anasontzis, G.E., Karlström, K., Larsson, P.T., Olsson, L., 2014. Morphology and enzyme
605 production of *Trichoderma reesei* Rut C-30 are affected by the physical and structural
606 characteristics of cellulosic substrates. *Fungal Genetics and Biology* 72, 64–72.
607 10.1016/j.fgb.2014.07.011.

608 Peterson, R., Nevalainen, H., 2012. *Trichoderma reesei* RUT-C30 – thirty years of strain improvement.
609 *Microbiology* 158, 58–68. 10.1099/mic.0.054031-0.

610 Pickart, C.M., 1999. Ubiquitin and the stress response, in: Latchman, D.S. (Ed.), *Stress Proteins:*
611 *Handbook of Experimental Pharmacology.* Springer-Verlag, Berlin, Heidelberg, 133–152.

612 Quintanilla, D., Hagemann, T., Hansen, K., Gernaey, K.V., 2015. Fungal morphology in industrial
613 enzyme production- Modelling and monitoring. *Advances in biochemical*
614 *engineering/biotechnology* 149, 29–54. 10.1007/10_2015_309.

615 Raggam, R.B., Salzer, H.J.F., Marth, E., Heiling, B., Paulitsch, A.H., Buzina, W., 2011. Molecular
616 detection and characterisation of fungal heat shock protein 60. *Mycoses* 54, 394-399.
617 10.1111/j.1439-0507.2010.01933.x.

618 Reese, E.T., Ryu, D.Y., 1980. Shear inactivation of cellulase of *Trichoderma reesei*. *Enzyme Microb.*
619 *Technol.* 2, 239–240.

620 Rocha-Valadez, J., Galindo, E., Serrano-Carreón, L., 2007. The influence of circulation frequency on
621 fungal morphology: dissipation rate cultures of *Trichoderma harzianum*. *J. Biotechnol.* 130 (4),
622 394–401. 10.1016/j.jbiotec.2007.05.001.

623 Roller, C., Maddalo, D., 2013. The molecular chaperone GRP78/BiP in the development of
624 chemoresistance: mechanism and possible treatment. *Front. Pharmacol.* 4, e00010, 1–5.
625 10.3389/fphar.2013.00010.

626 Shang, F., Taylor, A., 2011. Ubiquitin-proteasome pathway and cellular responses to oxidative stress.
627 *Free Radic. Biol. Med.* 51, 5–16. 10.1016/j.freeradbiomed.2011.03.031.

628 Soni, S.K., Sharma, A., Soni, R., 2018. Cellulases: Role in lignocelulosic biomass utilization, in: Lübeck,
629 M. (Ed.), *Cellulases.* Humana Press, New York, NY.

630 Stappler, E., Walton, J.D., Beier, S., Schmoll, M.A., 2017. Abundance of secreted proteins of
631 *Trichoderma reesei* is regulated by light of different intensities. *Front. Microbiol.* 8, e02586, 1–
632 14. 10.3389/fmicb.2017.02586.

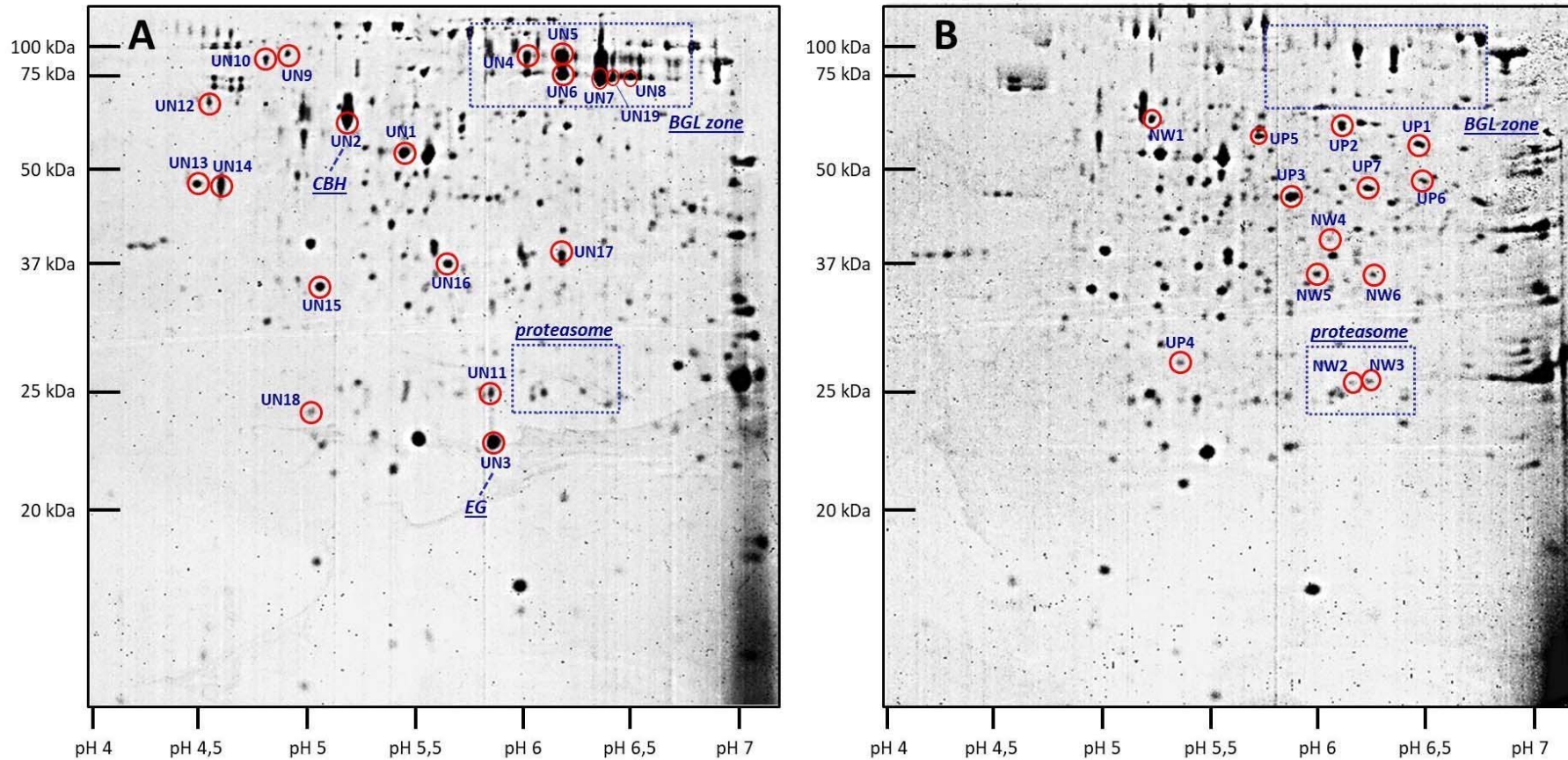
633 Staszczak, M., 2008. The role of the ubiquitin-proteasome system in the response of the ligninolytic
634 fungus *Trametes versicolor* to nitrogen deprivation. *Fungal Genetics and Biology* 45, 328–337.
635 10.1016/j.fgb.2007.10.017.

636 Tiwari, S., Thakur, R., Shankar, J., 2015. Role of heat-shock proteins in cellular function and in the
637 biology of fungi. *Biotechnol. Res. Int.*, 1–11. 10.1155/2015/132635.

638 Wang, Y., Delettre, J., Corrieu, G., Béal, C., 2011. Starvation induces physiological changes that act on
639 the cryotolerance of *Lactobacillus acidophilus* RD758. Biotechnol. Prog. 27 (2), 342–350.
640 10.1002/btpr.566.
641

642 **Supplementary material**

643 **Figure 1** : Proteomic analysis of *T. reesei* cells: A) 800 rpm ($EDCF_{\text{emax}} 1884 \text{ kW}\cdot\text{m}^{-3}\cdot\text{s}^{-1}$); B) 1700 rpm ($EDCF_{\text{emax}} 38400 \text{ kW}\cdot\text{m}^{-3}\cdot\text{s}^{-1}$); UN1-UN19:
644 under-synthesized proteins; UP1-UP7: over-synthesized proteins; NW1-NW6: newly-synthesized proteins.



645